SUPPORTING INFORMATION

Structural and Proton Conductivity Studies of Fibrous π-$Ti_2O(PO_4)_2 \cdot 2H_2O$: Application in Chitosan-Based Composite Membranes

Artem A. Babaryk,[a] Alaa Adawy,[b] Inés García,[c] Camino Trobajo,[d] Zakariae Amghouz,[e] Rosario M. P. Colodrero,[f] Aurelio Cabeza,[f] Pascual Olivera-Pastor,[f] Montse Bazaga-García*[f] and Lucía dos Santos-Gómez*[a]*

[a] Department of Physical and Analytical Chemistry, University of Oviedo – CINN (CSIC), 33006-Oviedo, Spain. E-mail: ldsg@uniovi.es; artem.babaryk@gmail.com

[b] Laboratory of HRTEM, Institute for Scientific and Technological Resources, University of Oviedo, 33006, Oviedo, Spain.

[c] Nanomaterials and Nanotechnology Research Centre – CINN (CSIC), 33940 El Entrego, Asturias, Spain.

[d] Department of Organic and Inorganic Chemistry, University of Oviedo – CINN (CSIC), 33006-Oviedo, Spain.

[e] Department of Materials Science and Metallurgical Engineering, University of Oviedo, 33203, Gijón, Spain.

[f] Universidad de Málaga, Dpto. de Química Inorgánica, Cristalografía y Mineralogía, 29071-Málaga, Spain.

E-mail: m.bazaga@uma.es

Table of Contents

Full Details of the DFT Calculations

Initial coordinates of atoms in the unit cell were taken from PXRD-refined crystal structures and used for further optimizations. Generalized gradient approximation of DFT in pristine Perdew-Becke-Ernzerhof (PBE)[1] and revised for solids (PBEsol)[2] parametrizations were applied to account for electron exchange and correlation. The valence electrons considered in the pseudopotentials for each atomic species are as follows: $3p^6 4s^2 3d^4$ for Ti, $3s^2 p^3$ for P, $2s^2 2p^4$ for O and $1s^1$ for H. The correction to the energies for London dispersion force was accounted utilizing the Tkachenko-Scheffler approach.[3] The plane-wave cutoff energy was set to be 520 eV. Brillouin zone sampling of electronic states was performed on 4×3×8 and 6×3×2 Monkhorst-Pack grids for $Ti_2O(H_2O)_2[PO_4]$ and $Ti_2O[PO_4]$, respectively. The structures were fully relaxed by the residual minimization method - direct inversion in the iterative space (RMM-DIIS),[4] after which the residual forces were converged to $< 10^{-2}$ eV Å^{-1} and free of Puley stress.

The calculation of magnetic response parameters were carried out using the gauge-including projector augmented wave (GIPAW) method[5,6] delivering the accuracy comparable to all-electron calculation for isolated and periodic boundary condition systems both equally ^{31}P NMR shifts were referenced to the absolute chemical shielding of H_3PO_4 (δ_{31P} = 0 ppm) standard sample. The latter was calculated for an isolated molecule in the box of 17×17×17 Å^3 using the same parameters as for π-TiP models.

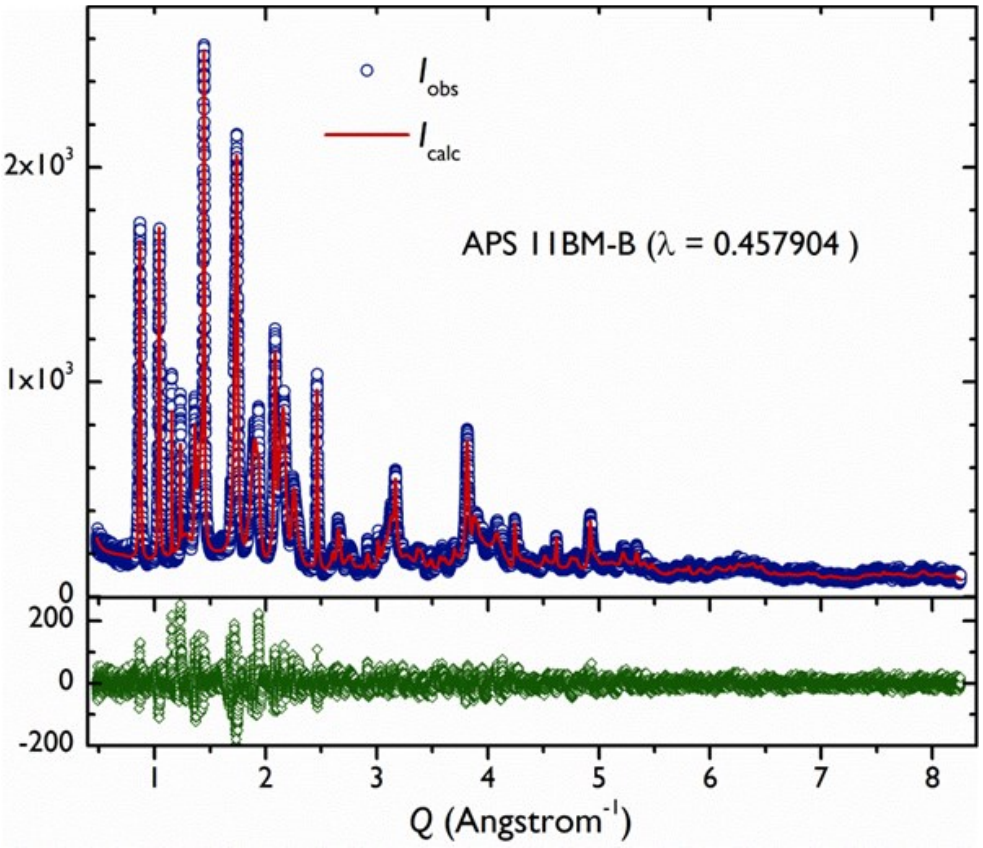

Figure S1. Final plot of the HR-PXRD profile after Rietveld refinements for **π-TiP_0** compound.

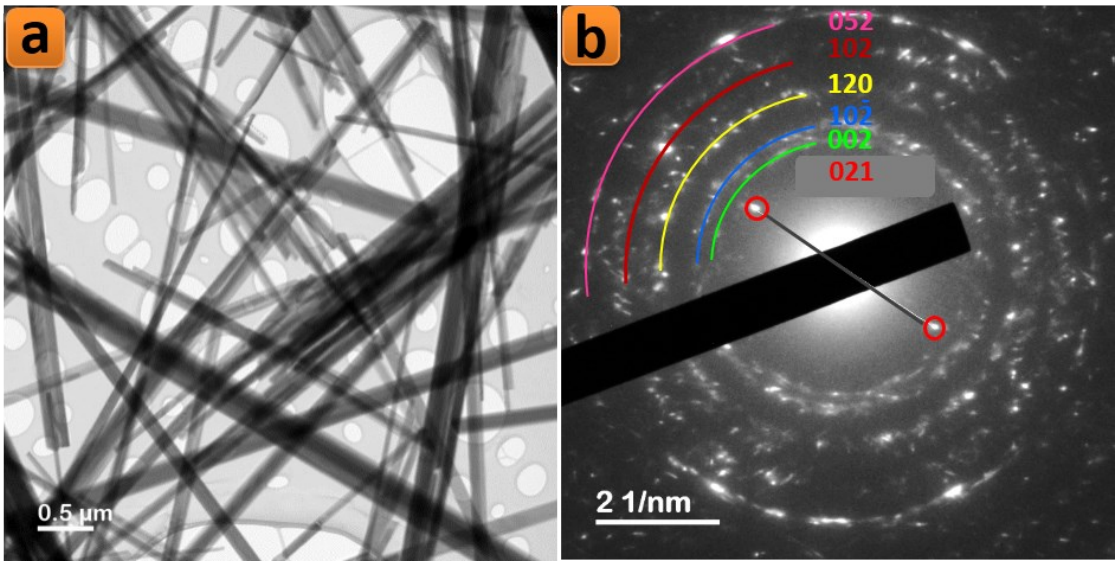

Figure S2. (a) BF-STEM image and (b) selected-area electron diffraction pattern of **π-TiP_0**.

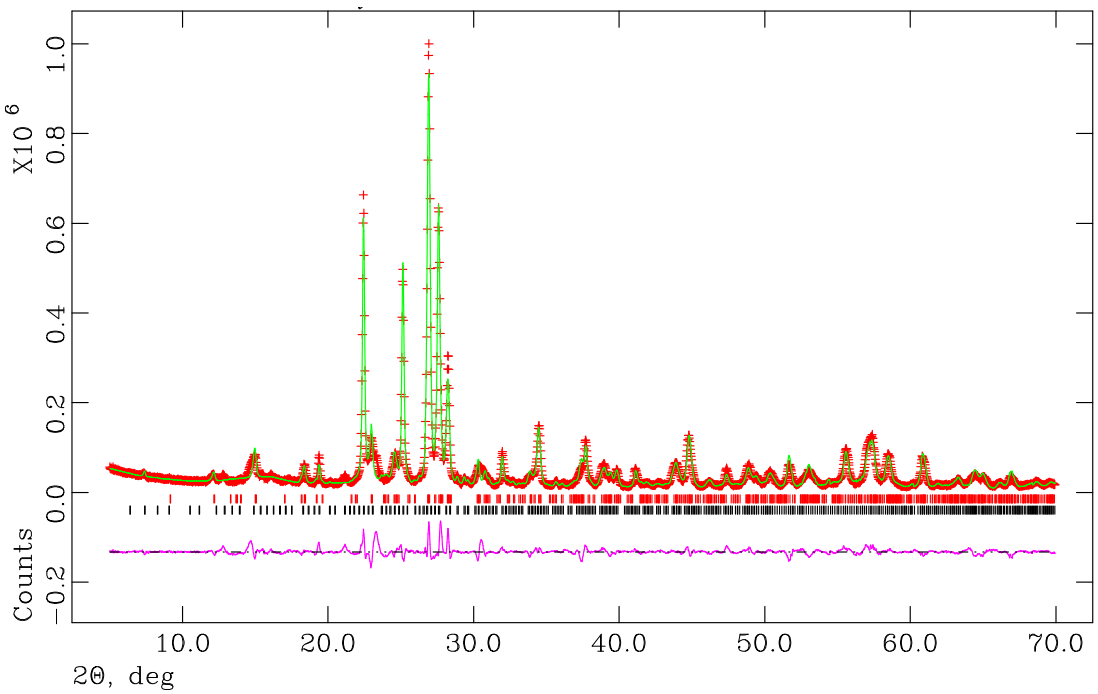

Figure S3. Rietveld plot for decomposition products at 900 ºC [black ticks: TiP_2O_7, red ticks: $Ti_5O_4(PO_4)_4$; R_{Wp} = 0.125; $R_F(TiP_2O_7)$ = 0.051; $R_F(Ti_5O_4(PO_4)_4)$ = 0.0421]

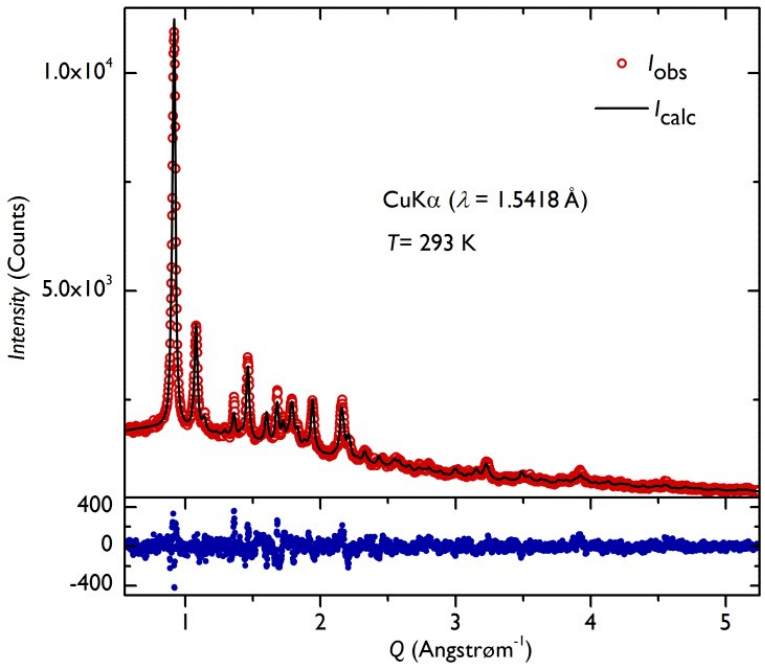

Figure S4. The final plot of the XRD profile after Rietveld refinements.

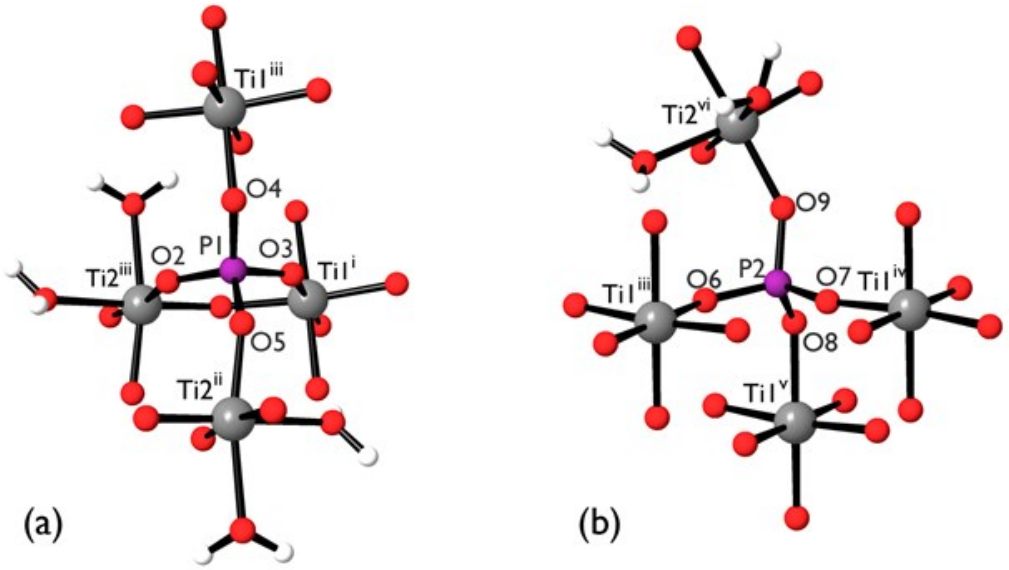

Figure S5. The local environment of P1 (a) and P2 (b) atoms (O, P and Ti atoms are depicted as red, violet and grey spheres). [Symmetry codes correspond to labels at the picture: (*i*) x,1/2−y, 1/2+z; (*ii*) −x,1/2+y, 1/2+z; (*iii*) 1−x, 1/2+y, 1/2−z; (*iv*) x, 1/2−y, 1/2+z; (*v*) −x, 1/2+y,1/2−z; (*vi*) 1−x, 1−y, −z].

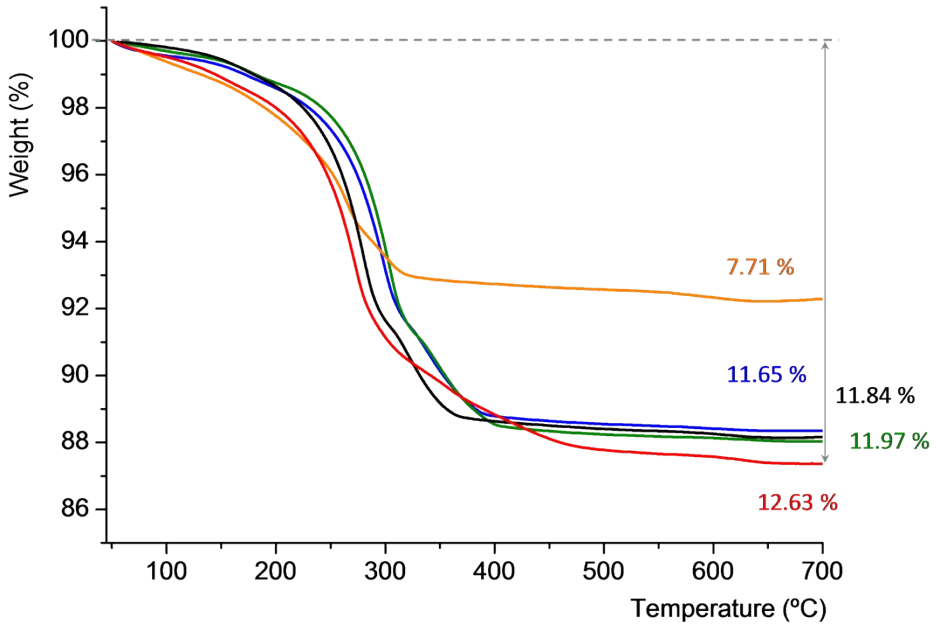

Figure S6. TGA curves comparison for π-TiP derivatives: as-synthetized **π-TiP_0** (blue), **π-TiP_0** after impedance (red), after washed treatment **π-TiP_10** (green), **π-TiP_10** partially rehydrated (orange), **H_3PO_4@π-TiP_10** (black).

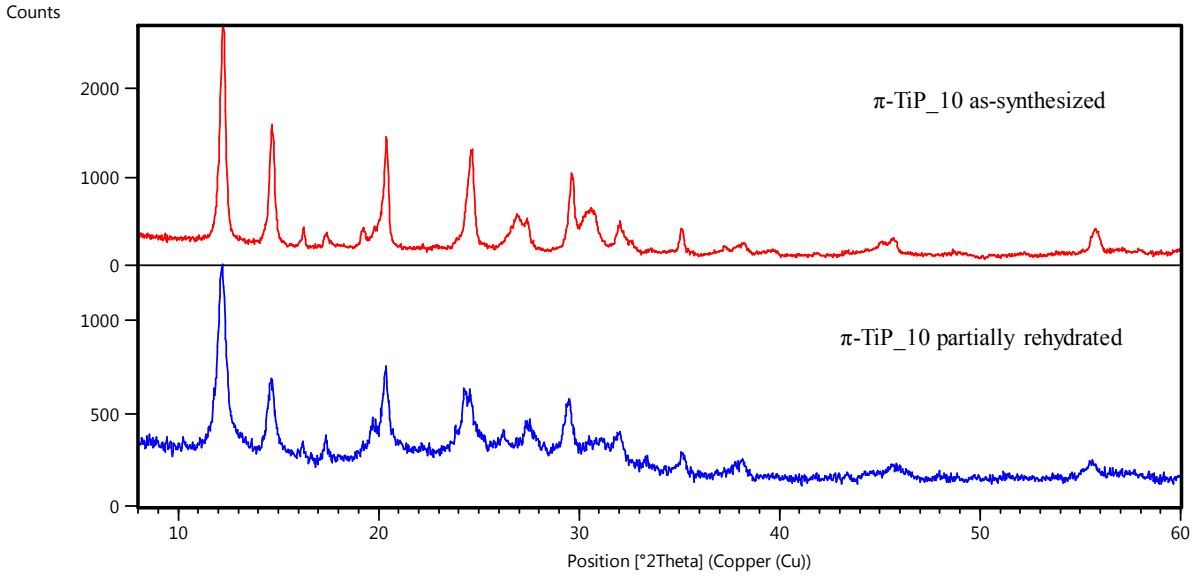

Figure S7. PXRD pattern for partially rehydrated **π-TiP_10** (blue) and as-synthesized **π-TiP_10** compound (red)

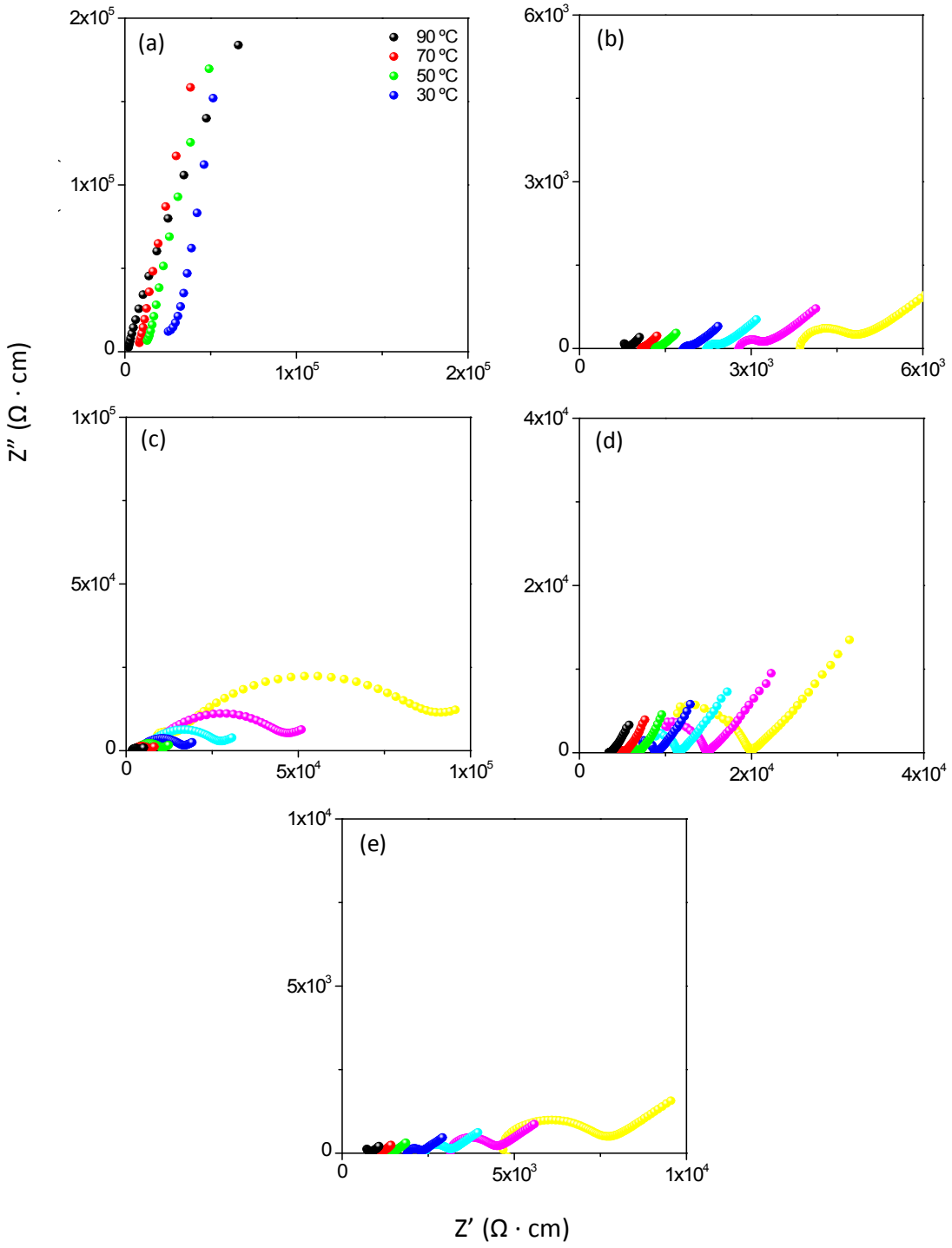

Figure S8. Plots of the complex impedance plane for (a) **π-TiP_0**, (b) **π-TiP_4**, (c) **π-TiP_10**, (d) **π-TiP_10** partially rehydrated and (e) **H_3PO_4@π-TiP_10** materials at 95% RH and different temperatures: 90 (black), 80 (red), 70 (green), 60 (blue), 50 (cyan), 40 (magenta) and 30 °C (yellow).

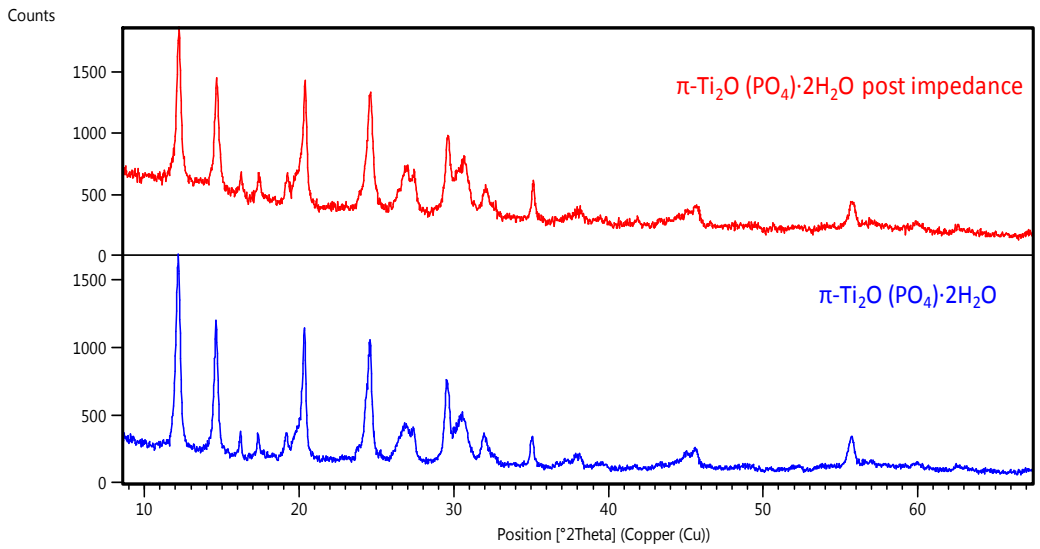

Figure S9. PXRD pattern comparison of π-$Ti_2O(PO_4)_2 \cdot 2H_2O$ (**π-TiP_0)** as synthetized (blue) and post impedance (red) compounds.

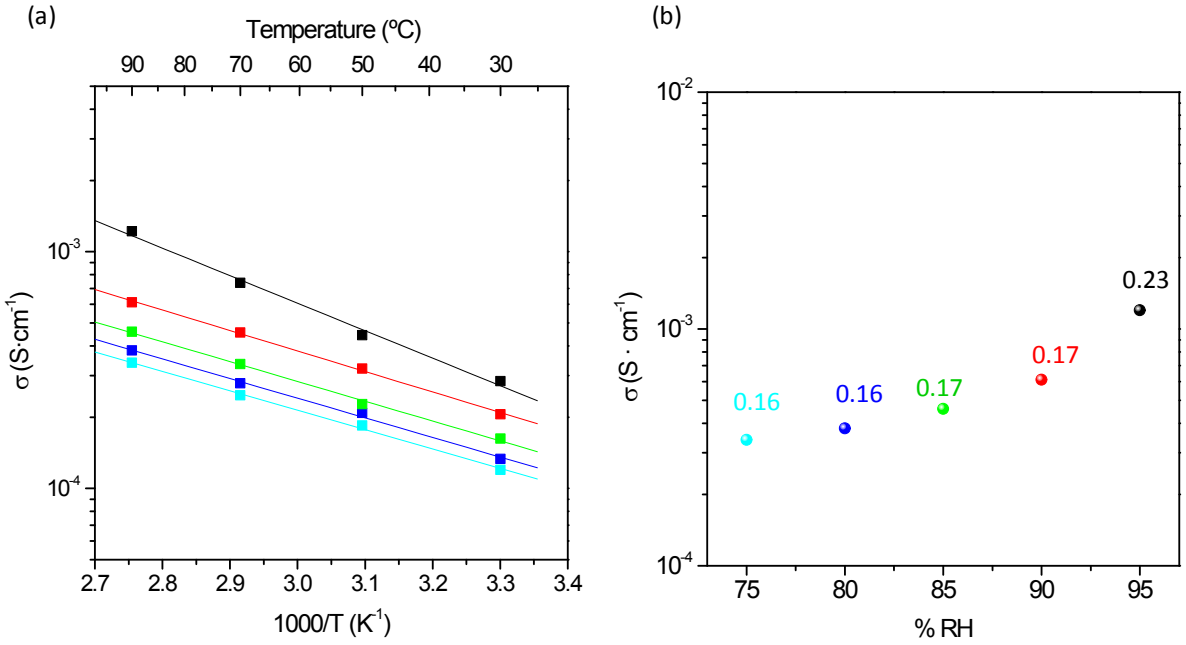

Figure S10. Impedance studies for **π-TiP_0**: (a) Conductivity values as function of temperature (Arrhenius plot) at different relative humidity: 95 (cyan), 90 (blue), 85 (green), 80 (red) and 75% RH (black); (b) Proton conductivity, at 90 °C, vs. % RH with activation energy values (Ea, eV) .

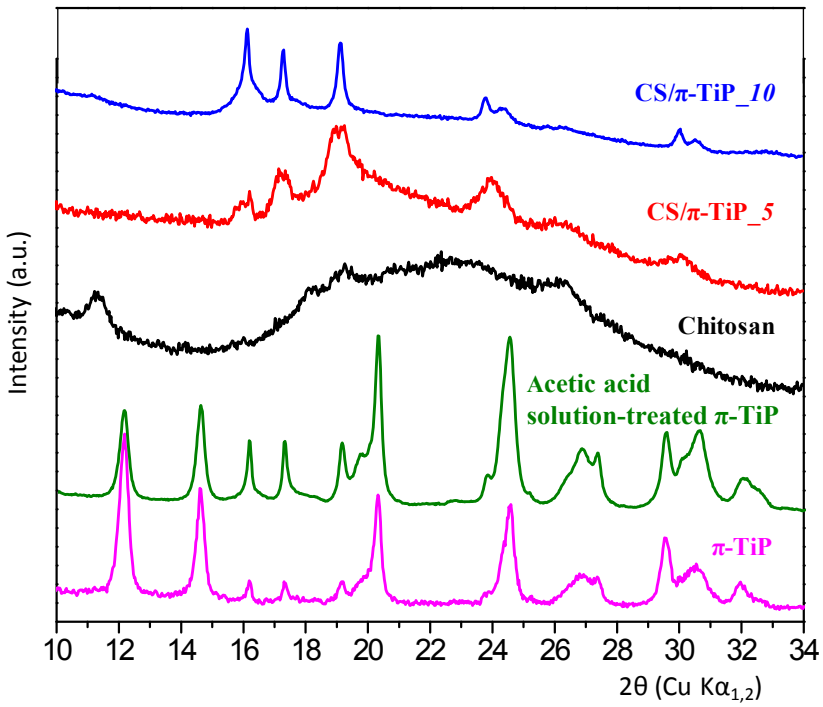

Figure S11. Comparison of PXRD pattern of **π-TiP_0** (magenta), **π-TiP** after immersing in an acetic acid solution (green), **CS** (black), **CS/π-TiP_*5*** (red) and **CS/π-TiP_*10*** (blue) membranes.

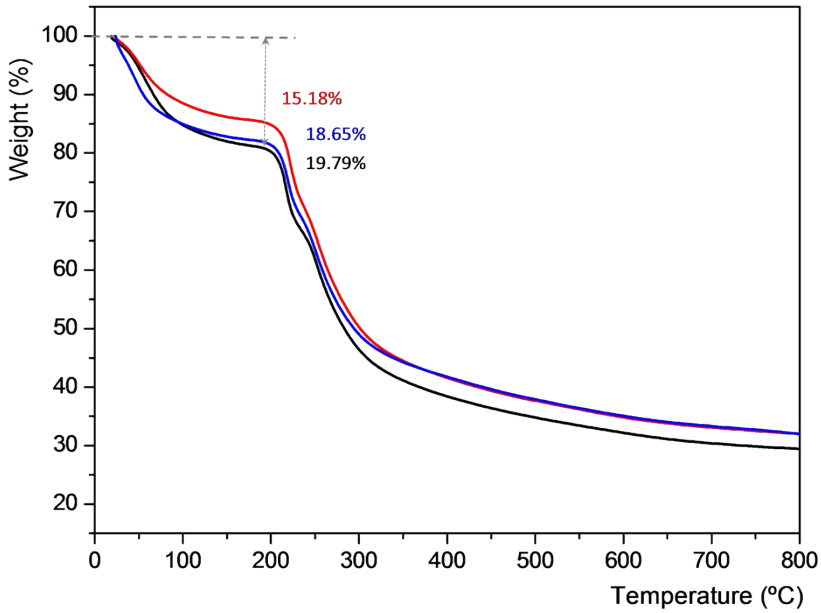

Figure S12. Comparison of TG analyses of **CS** (black), **CS/π-TiP-*5*** (red) and **CS/π-TiP-*10*** (blue) membranes.

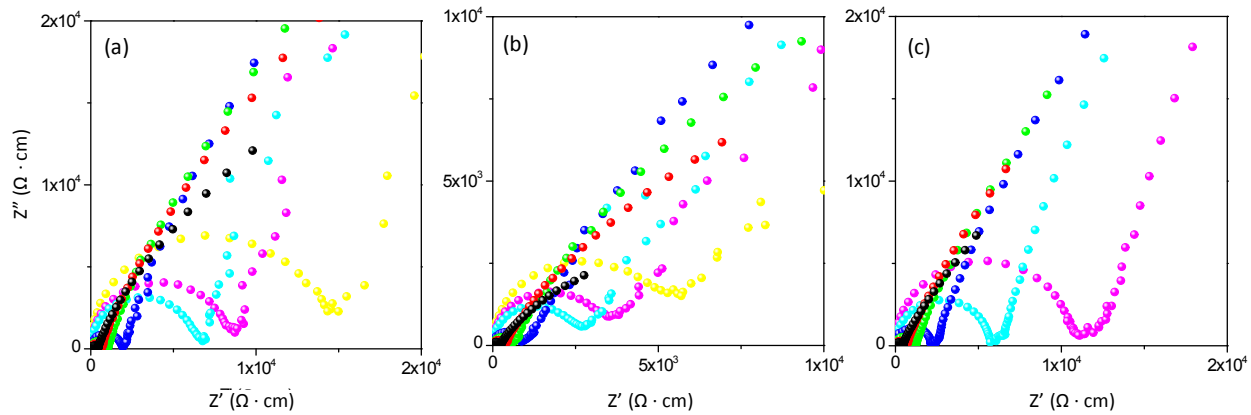

Figure S13. Plots of the complex impedance plane for (a) **CS** (black), **CS/π-TiP-*5*** (red) and **CS/π-TiP-*10*** (blue) membranes at 95% RH and differences temperatures: 80 (black), 70 (red), 60 (green), 50 (blue), 40 (cyan), 30 (magenta) and 25 °C (yellow).

Table S1. Selected parameters of the Rietveld refinements of the $Ti_2O(PO_4)_2 \cdot 2H_2O$ (**π-TiP_0**) structure from SR-PXRD data.

Parameter	**π-TiP_0**
T (K)	100
Space group	$P2_1/c$
a, b, c (Å)	5.1121(2), 14.4921(9), 12.0453(11)
β (deg)	115.31(1)
Z	4
Cell volume (Å^3)	806.74(11)
Calcd density (g cm^{-3})	2.784
Radiation wavelength (Å)	0.457904
R_p, R_{wp}, χ^2	0.062, 0.083, 1.347

$R_p = (\Sigma|Y_{o,m}-Y_{c,m}|)\ (\Sigma Y_{o,m})^{-1}$, $R_{wp} = \{\Sigma w_m(Y_{o,m}-Y_{c,m})^2\ (\Sigma w_m Y_{o,m}^2)\}^{1/2}$, $\chi^2=\{w_m(Y_{o,m}-Y_{c,m})^2\ (M-P)^{-1}\}^{1/2}$, where where $Y_{o,m}$ and $Y_{c,m}$ are the observed and calculated data respectively at data point m, M the number of data points, P the number of parameters, wm the weighting given to data point m which for counting statistics is given by $w_m=\sigma(Y_{o,m})^{-2}$ where $\sigma(Y_{o,}m)$ is the error in $Y_{o,m}$.

Table S2. Selected interatomic distances for the $Ti_2O(PO_4)_2 \cdot 2H_2O$ (**π-TiP_0**) structure.

Bond	Length (Å)	Bond	Length (Å)
Ti1–O1	1.9045(2)	Ti2–O1	1.8083(2)
Ti1–O3	1.9517(2)	Ti2–O2	2.0630(2)
Ti1–O6	2.0380(2)	Ti2–O10	2.2484(2)
Ti1–O7	1.9065(2)	Ti2–O11	2.1704(2)
Ti1–O8	1.9742(2)	Ti2–O5	1.9427(2)
Ti1–O4	2.0251(2)	Ti2–O9	1.9687(2)
P1–O2	1.5928(1)	P2–O6	1.5761(1)
P1–O3	1.5524(1)	P2–O9	1.5445(1)
P1–O4	1.5279(1)	P2–O8	1.5289(1)
P1–O5	1.5767(1)	P2–O7	1.5004(1)

Table S3. Crystallographic summary of the of the $Ti_2O(PO_4)_2$ (**π-TiP_500**) structure determined from HT-PXRD.

Parameter	π-TiP_500
T (K)	773
Space group	$P2_1/c$
a, b, c (Å)	5.1187(13), 11.0600(21), 14.4556(26)
β (deg)	107.645(17)
Z	4
Cell volume (Å^3)	779.87(29)
Calcd density (g cm^{-3})	2.569
Radiation wavelength (Å)	1.54178
R_p, R_{wp}, χ^2	0.030, 0.040, 1.377

Table S4. Selected interatomic distances for the $Ti_2O(PO_4)_2$ (**π-TiP_500**) structure.

Bond	Lengths (Å)	Bond	Length (Å)
Ti1–O1	1.8529(5)	Ti2–O7	1.8461(5)
Ti1–O5	1.9112(5)	P1–O1	1.4649(4)
Ti1–O6	1.9680(5)	P1–O2	1.5990(4)
Ti1–O8	1.8711(5)	P1–O3	1.5864(4)
Ti1–O9	1.9166(5)	P1–O4	1.5207(4)
Ti1–O4	1.9827(5)	P2–O5	1.6036(4)
Ti2–O2	1.7865(5)	P2–O7	1.5133(4)
Ti2–O9	1.7352(4)	P2–O6	1.6122(4)
Ti2–O3	1.8802(5)	P2–O8	1.4207(4)

Table S5. Unit cell parameters and fractional atomic coordinates of π-TiP after structure relaxation.

Space group – ***P*2$_1$/*c***, *a* = **5.1213 Å**, ***b*** **= 14.4099 Å,** *c* = **11.9312 Å**, ***β*** **= 115.0030º**, ***V*** **= 797.9771 Å^3**			
Atom	***x/a***	***y/b***	***z/c***
Ti1	0.04817	0.04311	0.30931
Ti2	0.55189	0.16843	0.05467
O1	0.13888	0.63132	0.31579
O2	0.33562	0.06062	0.06820
O3	0.30515	0.47449	0.24299
O4	0.16260	0.53572	0.70233
O5	0.64404	0.38551	0.42981
O6	0.41034	0.11676	0.35764
O7	0.77071	0.46112	0.05294
O8	0.05553	0.63120	0.08114
O9	0.72664	0.28733	0.04314
O10	0.37251	0.23847	0.16693
O11	0.15406	0.29607	0.39917
P1	0.61089	0.47295	0.35101
P2	0.28906	0.62350	0.03145
H1	0.04365	0.23863	0.39655
H2	0.02025	0.34765	0.35972
H3	0.37620	0.19940	0.23630
H4	0.17415	0.26220	0.12712

Table S6. The unit cell parameters and fractional atomic coordinates of **π-TiP-500** after structure relaxation.

***Space group* – *P*2$_1$/*c*, *a* = 5.1509 Å, *b* = 11.05990 Å, *c* = 14.48890 Å, *β* = 107.7990°, *V* = 785.9015 Å^3**			
Atom	***x/a***	***y/b***	***z/c***
Ti1	0.28690	0.18433	0.05099
Ti2	0.14993	0.44849	0.15506
P1	0.28971	0.66028	0.02744
P2	0.14062	0.53039	0.37344
O1	0.08082	0.76033	0.02030
O2	0.81837	0.42847	0.06144
O3	0.31439	0.58251	0.11937
O4	0.43069	0.20740	0.46865
O5	0.23973	0.44151	0.45741
O6	0.13843	0.08336	0.13237
O7	0.11001	0.46121	0.27694
O8	0.64874	0.13178	0.11840
O9	0.31456	0.31824	0.13959

Table S7. Calculated isotropic and anisotropic characteristics of ^{31}P chemical shift tensor for π-TiP.

Compound	δ_{iso}	Ω	κ
H_3PO_4	−292.75	112.48	0.49
π-TiP	−306.19	34.54	−0.27
	−317.97	11.98	0.19

Table S8. ^{31}P NMR shifts (ppm) and NMR-MAS percentage of surface protonated phosphate species (H_3PO_4, $H_2PO_4^-$, HPO_4^{2-}) for selected π-TiP derivatives.

Sample	**H_3PO_4**		**$H_2PO_4^-$**		**HPO_4^{2-}**		**PO_4^{3-}**	
π-TiP_0	- 0.079 (5.80)	0.370 (8.37)	- 5.382 (3.00)	- 7.00 (7.47)	- 17.34 (1.29)	- 18.82 (9.04)	- 11.923 (37.29)	- 25.221 (27.73)
π-TiP_4	- 0.079 (1.84)	-	- 5.06 (5.41)	- 6.80 (7.30)	- 17.34 (5.77)	- 18.82 (7.89)	- 11.923 (40.59)	- 25.221 (31.21)
π-TiP_6	- 0.079 (1.69)	-	- 5.78 (8.12)	-	-	- 18.28 (14.93)	- 11.923 (41.27)	- 25.221 (33.99)
π-TiP_10	- 0.079 (1.65)	-	- 5.78 (7.75)	-	-	- 17.97 (15.42)	- 11.923 (40.82)	- 25.221 (34.37)
H_3PO_4@π-TiP_10	- 0.079 (1.87)	-	- 4.87 (2.78)	- 6.69 (8.24)	- 17.63 (4.34)	- 18.82 (8.43)	- 11.923 (42.14)	- 25.221 (32.20)

REFENCES:

(1) Perdew, J. P.; Burke, K.; Ernzerhof, M. Generalized Gradient Approximation Made Simple. *Phys. Rev. Lett.* **1996**, *77*, 3865.

(2) Perdew, J. P.; Ruzsinszky, A.; Csonka, G. I.; Vydrov, O. A.; Scuseria, G. E.; Constantin, L. A.; Zhou, X.; Burke, K. Restoring the Density-Gradient Expansion for Exchange in Solids and Surfaces. *Phys. Rev. Lett.* **2008**, *100*, 136406.

(3) Tkatchenko, A.; Scheffler, M. Accurate Molecular Van Der Waals Interactions from Ground-State Electron Density and Free-Atom Reference Data. *Phys. Rev. Lett.* **2009**, *102*, 073005.

(4) Pulay P. Convergence Acceleration of Iterative Sequences. The Case of SCF Iteration. *Chem. Phys. Lett.* **1980**, *73*, 393-398.

(5) Pickard, C. J.; Mauri F. All-electron Magnetic Response with Pseudopotentials: NMR Chemical Shifts. *Phys. Rev. B* **2001**, *63*, 245101.

(6) Yates, J. R.; Pickard, C. J. Mauri, F. Calculation of NMR Chemical Shifts for Extended Systems Using Ultrasoft Pseudopotentials. *Phys. Rev. B* 2007, *76*, 024401.